

A Surrogate-Assisted Teaching-Learning-Based Optimization for Parameter Identification of The Battery Model

Yu Zhou, Bing-Chuan Wang, Han-Xiong Li, *Fellow, IEEE*, Hai-Dong Yang, and Zhi Liu

Abstract—Lithium-ion batteries are widely used as power sources in industrial applications. Electrochemical models and simulations are crucial to disclose many details that cannot be directly measured through experiments. Parameter identification of an accurate electrochemical model is much more cost-effective than direct and destructive measurement methods. However, the complex structure and strong nonlinearity of electrochemical models will make the parameter identification very difficult. Additionally, time-consuming electrochemical simulations can significantly limit the identification efficiency. This paper proposes a surrogate-model-based scheme to achieve high-efficiency parameter identification of an electrochemical battery model. To be specific, the proposed method is implemented by the close integration of an evolutionary algorithm and a surrogate model. A sensitivity-based identification strategy is first designed to alleviate the difficulty of optimization. Then, a surrogate model is developed from historical data to gradually approach the objective function used for parameter evaluations. Finally, an evolutionary algorithm is employed to find promising solutions by minimizing the output of the surrogate model. Simulations and experimental studies demonstrate the effectiveness and high efficiency of the proposed method.

Index Terms—Lithium-ion battery, parameter identification, evolutionary algorithm, surrogate model

I. INTRODUCTION

WITH the increasing depletion of fossil energy and environmental degradation, renewable energy has been rapidly developed. Lithium-ion batteries (LIBs) are widely used as power sources in industrial applications [1]. This success is mainly due to their high energy density, tiny memory effect, and long cycling life [2]. However, the performance of a battery is limited by overheating and degradation, which may

This work was supported by the National Key R&D Program of China (2018YFB1308202) and a GRF project from Hong Kong SAR (CityU: 11210719). (Corresponding authors: Han-Xiong Li and Bing-Chuan Wang.)

Yu Zhou is with the School of Mechanical and Electrical Engineering, Central South University, Changsha 410083, China, and also with the Department of Systems Engineering and Engineering Management, City University of Hong Kong, Kowloon, Hong Kong (e-mail: yuzhou@csu.edu.cn)

B.-C. Wang is with the School of Automation, Central South University, Changsha 410083, China (email: bcwang@csu.edu.cn)

H.-X. Li is with the Department of Systems Engineering and Engineering Management, City University of Hong Kong, Kowloon, Hong Kong (e-mail: mehxi@cityu.edu.hk)

H.-D. Yang is with the Guangdong Engineering Research Center for Green Manufacturing & Energy Efficiency Optimization, Guangdong University of Technology, Guangzhou 510006, China (e-mail: yanghd@yeah.net)

Zhi Liu is with the Guangdong-HongKong-Macao Joint Laboratory for Smart Discrete Manufacturing, Guangzhou 510006, China, and also with the Key Laboratory of Intelligent Detection and the Internet of Things in Manufacturing, Ministry of Education, Guangzhou 510006, China. (e-mail: lz@gdut.edu.cn)

cause potential hazards [3]. Thus, battery management systems (BMSs) are indispensable for the regulation of batteries [4]. To design a BMS, the behavior and internal characteristics of a battery should be simulated and analyzed through a well-performed model. In general, LIB models include equivalent circuit models [5], electrochemical impedance spectrum models [6], electrochemical models (EMs) [7], and data-driven models [8]. EMs are known to have high simulation accuracy since they can reflect physical phenomena based on physical laws. Also, the parameters of EMs can be exactly matched with the actual physical parameters of batteries [9]. The pseudo-two-dimensional (P2D) model is one of the most representative EMs [10]. The P2D model governed by partial differential equations (PDEs) is highly complex and nonlinear. If the model parameters are properly specified, the internal characteristics of LIBs could be accurately investigated by electrochemical simulations.

During the last decades, many parameter identification methods have been proposed including least square methods [11], recursive least square methods [12], Gaussian-Newton methods [13], Levenberg-Marquardt methods [14], and evolutionary algorithms (EAs) [15], [16].

If gradient-based methods are adopted for parameter identification and error minimization in the rigorous P2D model, the following challenges may arise [17]:

- It is hard to identify a proper initial value.
- Appropriate step sizes are difficult to be determined.
- Simple closed-form objective functions may be unavailable.
- Local optima may seriously impede the optimization.

Although the ensemble Kalman filter can be used for parameter identification of high-order models [18], it may have two limitations. Firstly, the probability density function assumed by the ensemble Kalman filter is Gaussian. However, this assumption may not be satisfied for the parameter identification of the P2D model [19]. Additionally, filter divergence may cause fast-growing computational errors [20].

Recent years have witnessed an increasing interest in the topic of EAs [21]. For complex optimization problems, gradient-free EAs can be used without the closed-form expression of the objective function. From this perspective, EAs are exactly suitable for parameter identification of the P2D model with high complexity and strong nonlinearity. Rahman *et al.* used the particle swarm optimization (PSO) to estimate four main dynamic parameters of a LiCoO₂ battery [22]. Li *et al.* obtained 18 critical parameters

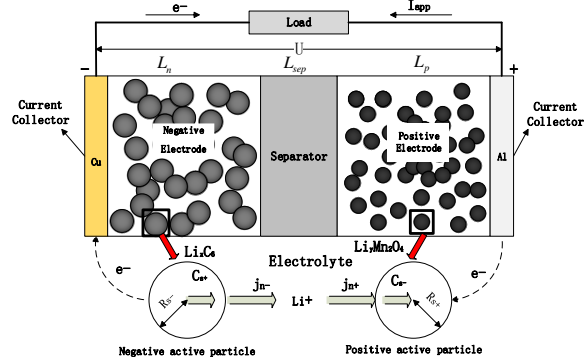


Fig. 1. Schematic of the P2D model.

of a LiMnO₄ battery using the genetic algorithm [17]. However, most studies use traditional EAs directly, which require a large number of simulation runs for parameter evaluations. Unfortunately, numerical simulations of the P2D model are computationally expensive. Thus, it is urgent to improve the computational efficiency of EAs. Conventionally, the computational efficiency is evaluated in terms of the computation time used to identify the parameters. Setting appropriate control parameters is another tricky issue for traditional EAs. Those control parameters can considerably affect the optimization results and tuning them is tedious. Thus, a teaching-learning-based optimization (TLBO) with a simple structure and few control parameters is adopted in this study.

Based on these observations, we propose a surrogate-assisted teaching-learning-based optimization (SA-TLBO) in this paper. In the proposed method, the TLBO is compactly combined with a data-based surrogate model to achieve efficient and accurate parameter identification of the complex P2D model. The main contributions of this paper are summarized as follows:

- A sensitivity-based identification strategy is designed to alleviate the difficulty of optimization and guarantee successful simulations.
- A surrogate model is developed to gradually approach the objective function by leveraging historical data.
- A TLBO is integrated with the surrogate model by which inferior solutions would be filtered out and thus computational efficiency can be improved.

The remainder of this paper is arranged as follows: The P2D model is described in Section II; The main techniques are discussed in Section III; Section IV shows the framework and procedures of the proposed method; Simulations and experimental validations are given in Section V; Section VI summarizes the conclusion.

II. PROBLEM DESCRIPTION

A. Pseudo-two-dimensional Model

As one of the most representative electrochemical LIB models, the P2D model has been thoroughly tested and validated [10]. As shown in Fig. 1, the behavior of porous electrodes is described by spherical particles surrounded by the

electrolyte. When a battery is working, the intercalation and de-intercalation of lithium-ions (Li⁺) are performed through the surface of particles. The P2D model involves a spatial dimension x between two electrodes and another dimension r inside particles. Since the dimension r is relatively small, this model cannot be strictly defined as a two-dimensional model. Thus, it is generally called the “pseudo-two-dimensional” model.

The P2D model is governed by a set of tightly coupled PDEs given in Table I. The specific meanings of the model parameters and variables can be seen in Table II. More details about the P2D model can be found in [23]. The terminal voltage is designated as the model output, which can be defined as follows:

$$\hat{U} = \varphi_s|_{x=0} - \varphi_s|_{x=L_p+L_{sep}+L_n} \quad (1)$$

B. Objective Function

For accurate simulations and analysis, a set of model parameters should be identified. The parameter identification can be formulated as the following optimization problem:

$$\min_{\vec{\theta}} \left\{ e(\vec{\theta}) : \vec{\theta} \in \mathbb{R}^d, p_i \in [LB_i, UB_i] \right\} \quad (2)$$

where $e(\vec{\theta}) : \mathbb{R}^d \mapsto \mathbb{R}^N$ represents the error between the model output voltages and the reference voltages; N is the number of data points; $\vec{\theta}$ denotes the parameter vector to be identified; p_i is one of the unknown parameters and $\vec{\theta} = (p_1, p_2, \dots, p_d)$; LB_i and UB_i are the lower and upper bounds of p_i ; d is the dimension of $\vec{\theta}$.

As the parameter identification can be formulated as an optimization problem, a feasible region, namely the solution space S that contains the optimal solution, should be set beforehand. By using the upper and lower bounds to define the range of a parameter, S can be expressed as the following Cartesian product [25], [26]:

$$S = \prod_{i=1}^d [LB_i, UB_i] \quad (3)$$

$$= \left\{ \vec{\theta} \in \mathbb{R}^d \mid LB_i \leq p_i \leq UB_i, i = 1, 2, \dots, d \right\}$$

In this paper, the error between the output voltages and the reference voltages is formulated as the objective (cost) function:

$$e(\vec{\theta}) = \| U^{ref} - \hat{U}(\vec{\theta}) \|_2 \quad (4)$$

where U^{ref} denotes the reference voltages. Some similar objective functions have been adopted by various methods [15], [22], [27].

III. SURROGATE-MODEL-ASSISTED EVOLUTIONARY OPTIMIZATION

For parameter identification of the P2D model, the following challenges may arise:

- Multi-scale characteristics of the model parameters increase the difficulty of parameter identification.

TABLE I
GOVERNING EQUATIONS OF THE P2D MODEL

Governing equations*	Boundary conditions
Electrodes	
$\frac{\partial C_{s,j}}{\partial t} + \frac{1}{r^2} \frac{\partial}{\partial r} (-D_{s,j} r^2 \frac{\partial C_{s,j}}{\partial r}) = 0$	$\left. \frac{\partial C_{s,j}}{\partial r} \right _{r=0} = 0$ $\left. D_{s,j} \frac{\partial C_{s,j}}{\partial r} \right _{r=R_j} = -J_j$
$\frac{\partial}{\partial x} \sigma_j^{eff} \frac{\partial \varphi_s}{\partial x} = a_j F J_j$	$\left. \frac{\partial \varphi_s}{\partial x} \right _{x=0} = -\frac{I}{\sigma_p^{eff}}$ $\left. \frac{\partial \varphi_s}{\partial x} \right _{x=L_p^-} = 0$ $\left. \frac{\partial \varphi_s}{\partial x} \right _{x=L_p + L_{sep}} = 0$ $\left. \frac{\partial \varphi_s}{\partial x} \right _{x=L_p + L_{sep} + L_n} = -\frac{I}{\sigma_n^{eff}}$
$\varepsilon_{e,j} \frac{\partial C_e}{\partial t} = \frac{\partial}{\partial x} (D_{e,j}^{eff} \frac{\partial C_e}{\partial x}) + a_j (1 - t_+) J_j$	$\left. \frac{\partial C_e}{\partial x} \right _{x=0} = \left. \frac{\partial C_e}{\partial x} \right _{x=L_p + L_{sep} + L_n} = 0$ $-D_{e,p}^{eff} \frac{\partial C_e}{\partial x} \Big _{x=L_p^-} = -D_{e,sep}^{eff} \frac{\partial C_e}{\partial x} \Big _{x=L_p^+}$ $-D_{e,sep}^{eff} \frac{\partial C_e}{\partial x} \Big _{x=L_p + L_{sep}^-} = -D_{e,n}^{eff} \frac{\partial C_e}{\partial x} \Big _{x=L_p + L_{sep}^+}$
$-\kappa_j^{eff} \frac{\partial \varphi_s}{\partial x} - \kappa_{e,j}^{eff} \frac{\partial \varphi_e}{\partial x} + \frac{2\kappa_{e,j}^{eff} RT}{F} (1 - t_+) \frac{\partial \ln C_e}{\partial x} = I$	$\left. \frac{\partial \varphi_e}{\partial x} \right _{x=0} = \left. \frac{\partial \varphi_e}{\partial x} \right _{x=L_p + L_{sep} + L_n} = 0$ $-\kappa_p \frac{\partial \varphi_e}{\partial x} \Big _{x=L_p^-} = -\kappa_{sep} \frac{\partial \varphi_e}{\partial x} \Big _{x=L_p^+}$ $-\kappa_{sep} \frac{\partial \varphi_e}{\partial x} \Big _{x=L_p + L_{sep}^-} = -\kappa_n \frac{\partial \varphi_e}{\partial x} \Big _{x=L_p + L_{sep}^+}$
Separator	
$\varepsilon_{e,sep} \frac{\partial C_e}{\partial t} = \frac{\partial}{\partial x} (D_{e,sep}^{eff} \frac{\partial C_e}{\partial x})$	$C_e \Big _{x=L_p^-} = C_e \Big _{x=L_p^+}$ $C_e \Big _{x=L_p + L_{sep}^-} = C_e \Big _{x=L_p + L_{sep}^+}$
$-\kappa_{e,sep}^{eff} \frac{\partial \varphi_e}{\partial x} + \frac{2\kappa_{e,sep}^{eff} RT}{F} (1 - t_+) \frac{\partial \ln C_e}{\partial x} = I$	$\varphi_e \Big _{x=L_p^-} = \varphi_e \Big _{x=L_p^+}$ $\varphi_e \Big _{x=L_p + L_{sep}^-} = \varphi_e \Big _{x=L_p + L_{sep}^+}$
Solid-liquid interface	
$J_j = k_j (C_{e,j})^{\alpha_{a,j}} (C_{s \max,j} - C_{s,e,j})^{\alpha_{a,j}} (C_{s,e,j})^{\alpha_{c,j}} [\exp(\frac{\alpha_{a,j} F}{RT} \eta_j) - \exp(-\frac{\alpha_{a,j} F}{RT} \eta_j)]$ $\eta_j = \varphi_{s,j} - \varphi_{e,j} - E_{ocv,j}$	

*Subscript j represents the positive electrode p or negative electrode n .

*Subscript sep represents the separator.

- Simulations of the P2D model are extremely time-consuming.
- Local optima may seriously impede the optimization.

To address these issues, the following three techniques are developed.

A. Sensitivity-Based Identification Strategy

1) *Parameter Classification*: The parameters to be estimated can be divided into two types: static parameters and dynamic parameters.

The static parameters based on the battery geometries and manufacturing processes are determined in the production process. If there are no pathological changes (e.g., severe overheating, excessive aging, and mechanical damage) inside a battery, the static parameters may not change significantly.

The dynamic parameters, which depend on the electrochemical properties of the battery materials, would vary with the change of lithium-ion concentration or reaction temperature in different operating modes. If a large external current is applied, the internal reactions would be accelerated and the polarization phenomena would be intensified. Subsequently, the dynamic parameters may change significantly and then cause severe effects on the output voltages.

The static parameters include the thickness of different regions, the radius of particles, the volume fraction, and the initial Li^+ concentration in electrolyte-phase. The dynamic parameters include the conductivity of electrodes, the diffusion coefficient in electrolyte-phase and solid-phase, the reaction rate coefficient of electrodes, and the Li^+ transference number [17]. The other related factors such as the maximum concentration of Li^+ and the equilibrium potential can be obtained from [28] and [29].

2) *Classified Identification Scheme*: Based on the previous discussion, the static and dynamic parameters can thus be identified by two specific operating modes, respectively. Some similar studies can be found in [17] and [30].

For the static parameters, a constant current corresponding to 0.01C can be used for identification. With such a small current, only slow electrochemical reactions occur inside the battery. Variations of the dynamic parameters may not cause obvious interference to the output voltages. Thus, the static parameters play a major role and can be identified first.

For the dynamic parameters, a constant current corresponding to 3C can be used for identification. With this relatively large current, the dynamic parameters gradually become sensitive due to rapid electrochemical reactions inside the battery. In this case, dynamic parameters play a dominant

TABLE II
PARAMETERS AND VARIABLES

Notation	Unit	Description [24]
L	m	Thickness
R	m	Radius of particles
ε_s	—	Volume fraction
ε_e	—	Volume fraction
C_{e0}	$mol\ m^{-3}$	Initial Li^+ concentration
σ	$S\ m^{-1}$	Conductivity of electrodes
D_e	$m^2\ s^{-1}$	Diffusion coefficient
D_s	$m^2\ s^{-1}$	Diffusion coefficient
k	$m^{2.5} mol^{-0.5} s^{-1}$	Reaction rate coefficient of electrodes
t_+	—	Li^+ transference number
σ^{eff}	$S\ m^{-1}$	Effective conductivity of electrodes
D_e^{eff}	$m^2\ s^{-1}$	Effective diffusion coefficient
C_e	$mol\ m^{-3}$	Li^+ concentration
r	m	Radial coordinate
x	m	Spatial coordinate
J	$mol\ m^{-2} s^{-1}$	Pore wall flux on particle surface
C_{s0}	$mol\ m^{-3}$	Initial Li^+ concentration in particles
C_{se}	$mol\ m^{-3}$	Li^+ concentration on particle surface
C_{smax}	$mol\ m^{-3}$	Maximum concentration of Li^+ in particles
a	m^{-1}	Specific surface area of particles
i_s	$A\ m^{-2}$	Current density
i_e	$A\ m^{-2}$	Current density
I	$A\ m^{-2}$	Total current density inside a battery
φ_s	V	Potential
φ_e	V	Potential
κ_e	$S\ m^{-2}$	Ionic conductivity
κ_e^{eff}	$S\ m^{-2}$	Effective ionic conductivity
α_a	—	Charge transfer coefficient of anode
α_c	—	Charge transfer coefficient of cathode
η	V	Over-potential
E_{ocv}	V	Equilibrium potential
\bar{U}	V	Terminal voltage
T	K	Temperature
\bar{R}	$J\ mol^{-1} K^{-1}$	Universal gas constant
F	$C\ mol^{-1}$	Faraday's constant
Subscript	—	Solid-phase
s	—	Electrolyte-phase

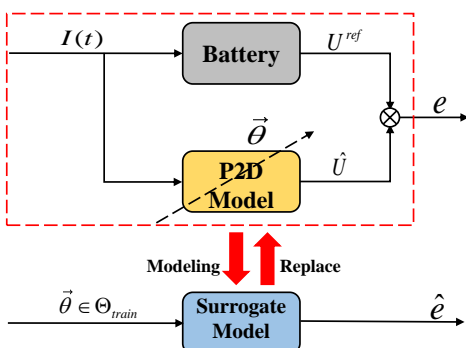


Fig. 2. Schematic of the surrogate modeling.

role and can be identified. Note that the previously identified static parameters can be directly used as known values.

3) *Effective Ranges of Model Parameters:* The P2D model is established in COMSOL Multiphysics using the battery module. Since unreasonable parameter values would cause unsuccessful simulations, the parameter ranges involving physical meanings should be set carefully. The effective bounds of the model parameters are mainly obtained from experiments and [17]. Setting details are given in Table III.

B. Surrogate-Model-Based Parameter Prescreening

To improve computational efficiency, a surrogate-model-based parameter prescreening is designed. Among various surrogate models, the Kriging model (also known as the Gaussian process) [31] is adopted in this paper. The main reason [32] is that the prediction uncertainty of the Kriging model has a good mathematical background, which can be used for prescreening methods [33] in surrogate-model-based optimization. The predictive distribution of the objective function value can be obtained from the Kriging model constructed by historical data. Afterward, the mean and variance of this distribution can be effectively used to guide the filling of new data.

As shown in Fig. 2, the candidate parameter vectors and the corresponding simulation errors are the input and output of the surrogate model, respectively. The surrogate model can approach the objective function gradually as the historical data increases. Consequently, it can be used to roughly evaluate the performance of candidate solutions. In this manner, inferior solutions can be filtered out without the P2D model simulations. The computation time of the data-based surrogate model can be almost ignored compared to the P2D model. Since the number of the P2D model simulations is significantly reduced, the computational efficiency of parameter identification can be considerably improved. Note that $\Theta_{train} = \{\vec{\theta}_1, \vec{\theta}_2, \vec{\theta}_3, \dots\}$ denotes the training solution group.

C. TLBO-Based Optimization

Since the P2D model has no simple closed-form expressions, gradient information of the objective function is unavailable. Thus, gradient-based methods could hardly be applied to identify the model parameters. Additionally, the optimization problem described in Eq. (2) may contain many local optima which can remarkably hinder the identification. In the proposed method, a gradient-free TLBO is employed to escape from local optima and approach the globally optimal solution.

The TLBO includes a teaching phase and a learning phase [34]. A brief description is shown as follows:

1) *Teaching Phase:* Each student represents a candidate solution $\vec{\theta}_i (i = 1, 2, \dots, NP)$. Students with initial information first learn from the teacher and then update their memories. This process can be formulated mathematically as follows:

$$\vec{\theta}_{i,new} = \vec{\theta}_{i,old} + rand \cdot (\vec{\theta}_{teacher} - T_F \cdot \vec{\theta}_{mean}) \quad (5)$$

where NP denotes the size of population (i.e., candidate solution group Θ_{candi}); $\vec{\theta}_{i,old}$ denotes the solution before learning; $\vec{\theta}_{i,new}$ represents the solution after updating; $rand$ is a random number uniformly distributed in $[0,1]$; $\vec{\theta}_{teacher}$ denotes the teacher (i.e., the best student so far). $\vec{\theta}_{mean}$ denotes the mean vector of all candidate solutions; T_F is a learning factor randomly assigned as 1 or 2.

2) *Learning Phase*: Each student $\vec{\theta}_i$ randomly learns from another student $\vec{\theta}_j$ and then updates memories. The updating rules can be expressed as follows:

$$\vec{\theta}_{i,new} = \begin{cases} \vec{\theta}_{i,old} + rand \cdot (\vec{\theta}_j - \vec{\theta}_{i,old}), & \text{if } f(\vec{\theta}_j) < f(\vec{\theta}_{i,old}) \\ \vec{\theta}_{i,old} + rand \cdot (\vec{\theta}_{i,old} - \vec{\theta}_j), & \text{if } f(\vec{\theta}_{i,old}) \leq f(\vec{\theta}_j) \end{cases} \quad (6)$$

IV. FRAMEWORK AND CRITICAL PROCEDURES

A. Framework Design

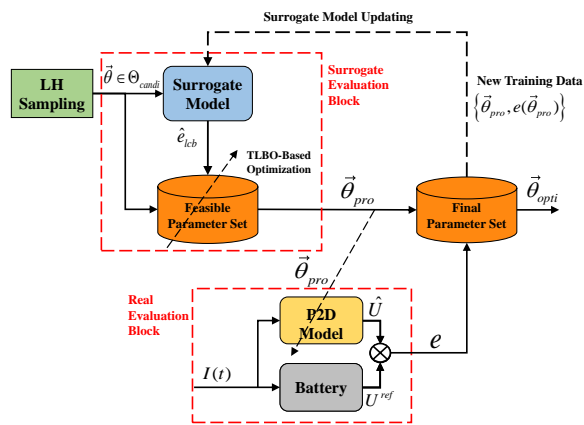


Fig. 3. Framework of the proposed SA-TLBO.

The framework of the proposed method is shown in Fig. 3. The Latin Hypercube Sampling (LHS) [35] is employed to generate the candidate solution group Θ_{candi} namely the feasible parameter set. LHS is a statistical method for generating a near-random sample of parameter values from a multi-dimensional distribution. Details can be found in [35], [36].

In the surrogate evaluation block, the TLBO is integrated with the surrogate model to optimize the feasible parameter set and filter out inferior candidate solutions. Given a new input solution $\vec{\theta}$ from Θ_{candi} , the predictive output \hat{E} of the Kriging model follows the Gaussian distribution [31]:

$$\hat{E} \sim N(\hat{e}(\vec{\theta}), s^2(\vec{\theta})) \quad (7)$$

where \hat{e} denotes the mean value; s is the standard deviation. For optimization algorithms using the Kriging model, many infill sampling criteria have been developed so far [37], [38]. As one of the most representative criteria, the lower confidence bound (LCB) criterion [39] is adopted in this study. To fully search the solution space with a balance between exploration and exploitation, the following LCB function is used as the objective function for the TLBO-based optimization.

$$\hat{e}_{lcb} = \hat{e} - \omega s \quad (8)$$

where ω is generally set to 2 [32]. After the surrogate evaluation, the promising solutions $\vec{\theta}_{pro}$ are collected to form the final parameter set.

In the real evaluation block, the promising solutions are evaluated by the P2D model simulations. Afterward, the data-pair $\{\vec{\theta}_{pro}, e(\vec{\theta}_{pro})\}$ can be added to the training solution group

Θ_{train} for surrogate model updating. Once the predefined termination conditions are met, the optimal solution $\vec{\theta}_{opti}$ can be obtained from the final parameter set.

To avoid being trapped in local optima and approach the globally optimal solution, the TLBO is applied for parameter identification. Traditional EAs update their memories by randomly recombining the candidate solutions stored in them. However, such an update mode requires a mass of simulation runs for candidate evaluations. If a computationally expensive model such as the P2D model is used, parameter identification using EAs would be time-consuming. Due to the surrogate-model-based parameter prescreening, the proposed method is more efficient than traditional EAs.

Remark 1. The two principal classes of system identification techniques are “parametric” and “non-parametric” identification methods [21], [40]. In this paper, a framework that integrates a heuristic algorithm and a surrogate model is proposed for accurate and efficient parameter identification. From this perspective, the proposed method might be considered as a kind of “parametric” identification method. Well-known “parametric” identification methods include least-square methods and maximum likelihood estimation, etc [21], [41]. Compared with the least-square methods, the proposed method can be used without a closed-form solution of the P2D model related to parameters. Compared with the maximum likelihood estimation, the proposed method does not rely on the likelihood function, which is difficult to construct while the complex P2D model is used.

B. Critical Procedures

As described in the framework, the optimal solution $\vec{\theta}_{opti}$ can be gradually approached by two-stage optimization. To specify the execution steps of the proposed method, a flowchart is given in Fig. 4. Additionally, the critical procedures are summarized as follows:

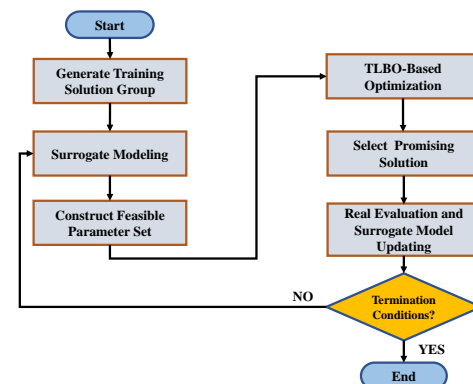


Fig. 4. Flowchart of the proposed SA-TLBO.

- S1:** Generate an initial training solution group Θ_{train} by the P2D model simulations.
- S2:** Construct the Kriging model using the training data.
- S3:** Generate a candidate solution group Θ_{candi} from the solution space S (described in Eq. (3)).
- S4:** Optimize the feasible parameter set based on the combination of the TLBO and the surrogate model.

- S5:** Obtain the promising solutions $\vec{\theta}_{pro}$ and establish a final parameter set.
- S6:** Evaluate $\vec{\theta}_{pro}$ by the P2D model simulations and infill new training data into Θ_{train} .
- S7:** If the final termination conditions are met, the best historical value of $\vec{\theta}_{pro}$ is taken as the optimal solution $\vec{\theta}_{opti}$; otherwise, return to **S2**.

V. VALIDATIONS AND DISCUSSIONS

A. Simulation-Based Validations

To validate the identified results directly, a simulation system of a 20Ah LiMn₂O₄ / Graphite pouch battery was established in the COMSOL Multiphysics. A set of reference parameters [17] were taken to generate reference voltages under different operating modes. The reference voltages under 0.01C and 3C were used to identify the static parameters and dynamic parameters, respectively. The identified results were validated by the reference voltages under 1C, 2C, and the Urban Dynamometer Driving Schedule (UDDS) mode.

The program was run in the MATLAB based on a workstation with Intel (R) Xeon (R) E5-1620 CPU and 8GB RAM. The specific settings of the proposed method are summarized as follows:

- Initial size of the training solution group Θ_{train} (mentioned in Fig. 2): $N_{t0} = 40$.
- Initial size of the candidate solution group Θ_{candi} (initial population size of the TLBO): $NP = 500$.
- The maximum number of iterations of the TLBO: $M_T = 200$.
- The maximum number of the P2D simulation runs for the entire identification: $M_R = 100$.
- Termination conditions of the TLBO-based optimization: the LCB function value $\hat{e}_{lcb} \leq 0.03$ (mentioned in Eq. (8)) or $M_T = 200$ is reached.
- Final termination conditions: the objective function value $e \leq 0.01$ (mentioned in Eq. (4)) or $M_R = 100$ is reached.

As shown in Table III, most of the identified parameters are close to the reference parameters. Note that the identified values of σ_p and σ_n are less accurate than others, which is possibly due to their low sensitivities to the output voltages. The conductivity of the electrode has special material properties. Only changes in conductivity exceeding 30-40 S/m can cause significant effects on the output voltages [42].

As shown in Figs. 5 - 6, the simulation data under 0.01C, 1C, 2C, and 3C show good agreement with the reference voltages. The input signals mentioned above are constant while the applied current used in practical applications is often randomly changed based on the practical scenario. Thus, we further investigated the performance of the identified results under the complex UDDS operating mode. As shown in Fig. 7, the identified parameters achieve encouraging performance. Table IV compares the proposed method with peer methods based on the computation time which is consumed to achieve the predefined accuracy on the training data. As shown in the table, peer methods require much more real evaluations and computation time than the proposed method. That is to

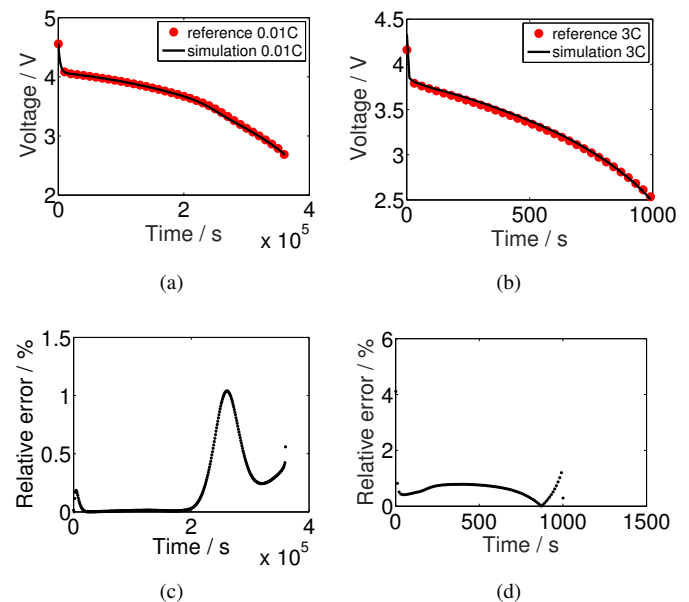


Fig. 5. Validation results of the proposed method using 0.01C and 3C reference voltages: (a) (b) voltage comparison, (c) (d) relative errors.

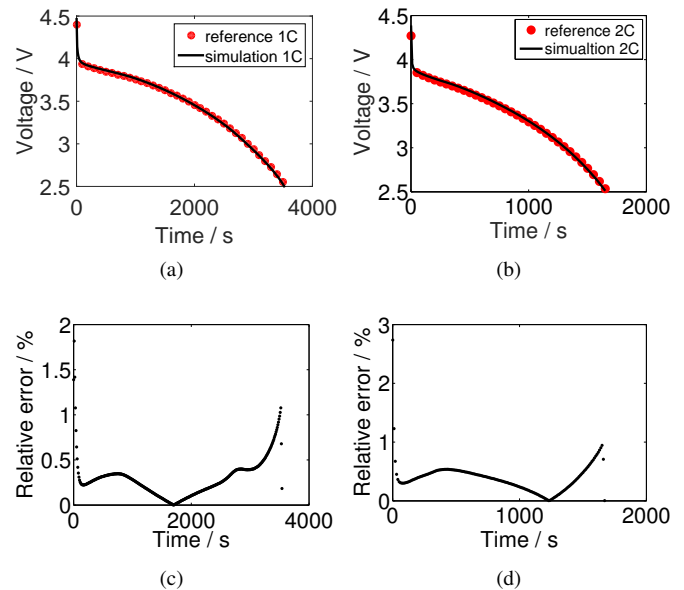


Fig. 6. Validation results of the proposed method using 1C and 2C reference voltages: (a) (b) voltage comparison, (c) (d) relative errors.

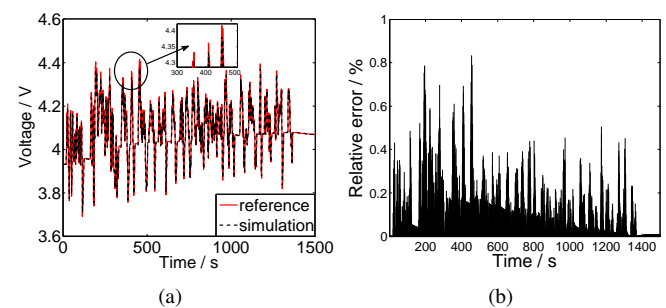


Fig. 7. Validation results of the proposed method using the UDDS reference voltages: (a) voltage comparison, (b) relative errors.

TABLE III
IDENTIFIED RESULTS FROM THE SIMULATION SYSTEM

Notation	Unit	Effective Ranges	Reference Values	Identified Results
Static Parameters				
L_p	m	[180e-6,197e-6]	183e-6	180.70e-6
L_{sep}	m	[50e-6,66e-6]	52e-6	53.581e-6
L_n	m	[92e-6,125e-6]	100e-6	104.32e-6
R_p	m	[5e-6,1e-5]	8e-6	6.9741e-6
R_n	m	[1e-5,1.6e-5]	1.25e-5	1.3730e-5
$\varepsilon_{s,p}$	—	[0.2,0.5]	0.297	0.2509
$\varepsilon_{s,n}$	—	[0.3,0.5]	0.477	0.4235
$\varepsilon_{e,p}$	—	[0.15,0.3]	0.259	0.2575
$\varepsilon_{e,n}$	—	[0.15,0.3]	0.172	0.2333
C_{e0}	$mol\ m^{-3}$	[1800,2200]	2000	1954.3
$C_{s0,p}$	$mol\ m^{-3}$	[2000,6500]	3900	4020.5
$C_{s0,n}$	$mol\ m^{-3}$	[8000,20000]	14870	14645.3
$C_{smax,p}$	$mol\ m^{-3}$	—	22860	22860
$C_{smax,n}$	$mol\ m^{-3}$	—	26390	26390
Dynamic Parameters				
σ_p	$S\ m^{-1}$	[1,50]	3.8	18.6395
σ_n	$S\ m^{-1}$	[90,200]	100	127.3387
D_e	$m^2 s^{-1}$	[1e-11,2e-10]	7.5e-11	7.5115e-11
$D_{s,p}$	$m^2 s^{-1}$	[5e-14,2e-13]	1e-13	8.5358e-14
$D_{s,n}$	$m^2 s^{-1}$	[3e-13,7e-13]	5e-13	5.3864e-13
k_p	$m^{2.5} mol^{-0.5} s^{-1}$	[8e-12,4e-11]	2e-11	1.7625e-11
k_n	$m^{2.5} mol^{-0.5} s^{-1}$	[8e-12,4e-11]	2e-11	2.0604e-11
t_+	—	[0.2,0.5]	0.363	0.3001

say, the proposed method is able to identify the parameters of the complex P2D model more quickly. Additionally, the proposed method was further compared with the peer methods according to the root mean square error (RMSE) and the mean absolute error (MAE) on the test data. As shown in Table V, the proposed method is more accurate than peer methods in terms of RMSE and MAE.

$$RMSE = \sqrt{\frac{1}{N} \sum_{i=1}^N (U_i^{ref} - \hat{U}_i)^2}$$

$$MAE = \frac{1}{N} \sum_{i=1}^N |U_i^{ref} - \hat{U}_i|$$

TABLE IV
COMPUTATION TIME OF DIFFERENT METHOD

The number of real evaluations		Computation time(s)
Static parameters		
Initial training data: 40		
Identification process: 53		
SA-TLBO	Dynamic parameters	4352
Initial training data: 40		
Identification process: 76		
Sum: 209		
TLBO	3360	69324
PSO	3802	80229

TABLE V
TEST ACCURACY OF DIFFERENT METHOD

	1C		2C		UDDS	
	RMSE	MAE	RMSE	MAE	RMSE	MAE
SA-TLBO	0.0154	0.0129	0.0198	0.0162	0.0489	0.0324
TLBO	0.0161	0.0146	0.0215	0.0181	0.0717	0.0522
PSO	0.0175	0.0137	0.0233	0.0199	0.0740	0.0580

B. Experiment-Based Validations

To validate the performance of the proposed method in the real world, some data were sampled from real experiments where a new 20Ah LiFePO₄ / Graphite pouch lithium-ion battery was used. The experimental configuration and the test bench can be seen in Figs. 8 - 9. Specifically, the battery test system (BTS) was employed to provide different operating modes. The thermal chamber was used to provide a stable ambient temperature. The measured data could be collected by the BMS. All these devices were integrated through a host computer. As with the simulation-based validations, the experimental voltages under 0.01C and 3C were used to identify parameters, while the remaining data were used for validations. Due to the complex dynamics of a real battery, the true parameter values are unknown in advance. Thus, the effective ranges of the model parameters were roughly set according to [43].

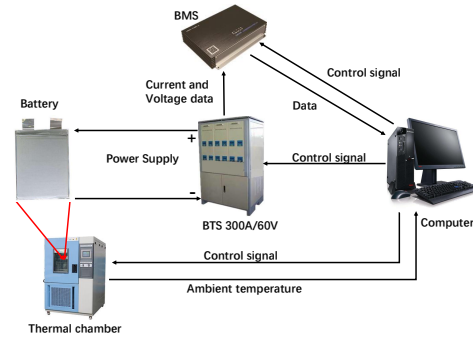


Fig. 8. Configuration of the experimental platform.



Fig. 9. The experimental test bench.

The identified parameter values based on experimental voltages are given in Table VI. Validation results of the proposed method using 0.01C, 1C, 2C, and 3C experimental voltages can be seen in Figs. 10 - 11. Despite the noticeable rising errors at the end of voltage curves, the relative errors are generally less than 6%. As shown in Fig. 12, the simulation voltages show good agreement with the experimental voltages under the UDDS mode and the relative errors are generally less than 5%.

C. Discussion of Results

Validation results suggest the outstanding performance of the proposed method both in the simulation system and experiments in terms of accuracy and efficiency. However,

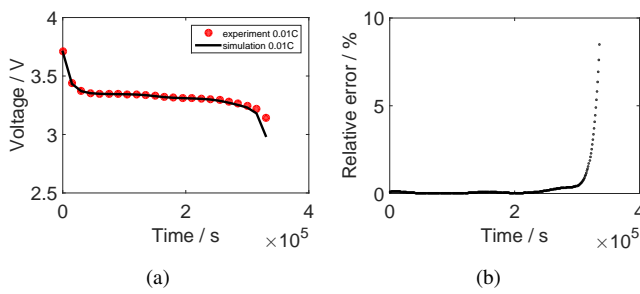


Fig. 10. Validation results of the proposed method using 0.01C experimental voltages: (a) voltage comparison, (b) relative errors

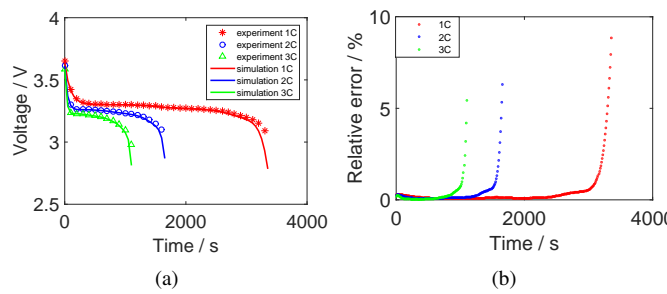


Fig. 11. Validation results of the proposed method using 1C, 2C, and 3C experimental voltages: (a) voltage comparison, (b) relative errors

the overall accuracy in the experimental study is lower than that in the simulation study. Additionally, the fitting errors of experimental voltages increase rapidly at the end of the voltage curves. Possible reasons for this may be battery degradation and unknown disturbances. The battery used in experiments may have capacity degradation resulted from the aging phenomenon. Since the P2D model cannot describe degradation without the aid of a thermal model [44], the loss of accuracy in capacity-related parameters may cause test errors.

As a heuristic algorithm, the TLBO can approach the globally optimal solution without being impeded by local optima. With the guidance of the surrogate model, inferior solutions can be filtered out by TLBO-based optimization. In this manner, only a few promising solutions are evaluated by the P2D model simulations. Since the number of simulation runs is considerably reduced, the proposed SA-TLBO requires much less computation cost compared with traditional EAs (i.e., PSO and TLBO).

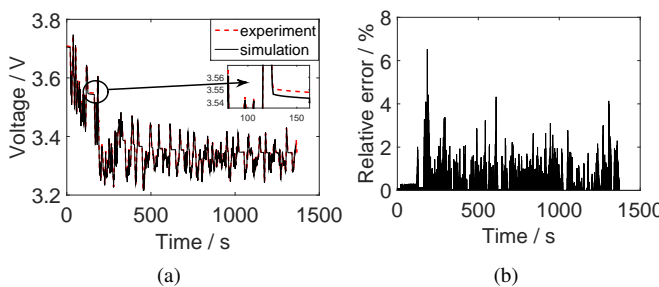


Fig. 12. Validation results of the proposed method using the UDDS experimental voltages: (a) voltage comparison, (b) relative errors

TABLE VI
IDENTIFIED RESULTS FROM EXPERIMENTS

Notation	Unit	Effective Ranges	Identified Results
Static Parameters			
L_p	m	[5e-5,9e-5]	7.1310e-5
L_{sep}	m	[1e-5,8e-5]	2.4730e-5
L_n	m	[1e-5,5e-5]	3.3460e-5
R_p	m	[1e-6,5e-6]	3.9621e-6
R_n	m	[1e-8,1e-7]	3.8620e-8
$\varepsilon_{s,p}$	—	[0.2,0.5]	0.4122
$\varepsilon_{s,n}$	—	[0.2,0.6]	0.5421
$\varepsilon_{e,p}$	—	[0.2,0.5]	0.3521
$\varepsilon_{e,n}$	—	[0.2,0.5]	0.3454
C_{e0}	$mol\ m^{-3}$	[1000,2000]	1236.5822
$C_{s0,p}$	$mol\ m^{-3}$	[100,1000]	462.2640
$C_{s0,n}$	$mol\ m^{-3}$	[1000,4000]	2697.4117
$C_{smax,p}$	$mol\ m^{-3}$	—	22860
$C_{smax,n}$	$mol\ m^{-3}$	—	26390
Dynamic Parameters			
σ_p	$S\ m^{-1}$	[1,50]	2.2138
σ_n	$S\ m^{-1}$	[80,200]	113.2568
D_e	$m^2 s^{-1}$	[1e-11,2e-10]	7.6253e-11
$D_{s,p}$	$m^2 s^{-1}$	[1e-13,5e-12]	1.3233e-12
$D_{s,n}$	$m^2 s^{-1}$	[1e-14,5e-14]	3.6254e-14
k_p	$m^{2.5} mol^{-0.5} s^{-1}$	[8e-12,4e-11]	1.8528e-11
k_n	$m^{2.5} mol^{-0.5} s^{-1}$	[8e-12,4e-11]	2.2257e-11
t_+	—	[0.2,0.5]	0.3411

Although the proposed method shows good performance under offline conditions, it owns a general drawback like various methods for parameter estimation of the P2D model [15], [16], [22], [27]. As the number of cycles increases, the parameters obtained offline may not adapt to the true physical parameters of the battery gradually. To tackle this issue, here are some potential solutions: a) Utilize various operating modes covering constant-current discharge, relaxation, different driving cycles, and different ambient temperatures to obtain a set of parameters offline. Then, the offline parameters can be used for real-time estimation in the framework of transfer optimization, which is a state-of-the-art approach using prior knowledge for highly efficient optimization [45]. b) Develop a computationally efficient reduced-order P2D model and integrate it with the surrogate model to perform online parameter estimation. Some further discussions can be found in the Appendix.

VI. CONCLUSION

An SA-TLBO method is proposed for parameter identification of the P2D model. The proposed method contains an optimization framework integrating a TLBO and a Kriging model. The gradient-free TLBO can generate promising solutions from numerous candidate solutions based on heuristic rules and avoid being trapped in local optima. The Kriging model constructed using historical data can evaluate the candidate parameters stored in the TLBO to filter out inferior solutions. Since only a small number of promising solutions are required to be evaluated by time-consuming simulations of the P2D model, the computational efficiency is significantly improved. Simulations and experiments show that the proposed method

is indeed effective and consumes much less computation time than traditional heuristic algorithms. In our future work, online parameter identification for a real-time system is under consideration.

APPENDIX

Remark A-1. The P2D model introduced in this paper is solved in COMSOL using the finite element method. Owing to the high complexity and strong nonlinearity of the P2D model, such a numerical simulation is very time-consuming. A single P2D model simulation takes about 20 seconds on our workstation. If the P2D model simulation must be performed for each evaluation of a candidate solution, the computational burden would be unaffordable.

In the proposed method, we used a data-based surrogate model to gradually approach the objective function. In this way, the surrogate model can be used to prescreen candidate parameters and significantly reduce the number of the P2D model simulations. The time required for a single computation of the surrogate model in MATLAB is about 0.01 seconds.

It can be found that the computational burden of the surrogate model can be almost ignored compared to the P2D model. Since the number of the P2D model simulations is significantly reduced, the computational efficiency of parameter identification can be considerably improved, as shown in the Table IV.

Remark A-2. Experiments have been performed on an aged LiFePO₄ battery that has been used for two years. As shown in the following figure, the discharge trajectories of this aged battery have changed significantly under operating modes of 0.5C, 1C, and 2C. The proposed method is used to identify the parameters of the P2D model based on the current state of health of the battery. In this paper, since a new battery is used to perform experiments, the identified parameters cannot be adapted to an aged battery. Fortunately, owing to the high computational efficiency of our method, we can conveniently reuse it for parameter identification of an aged battery according to its current state.

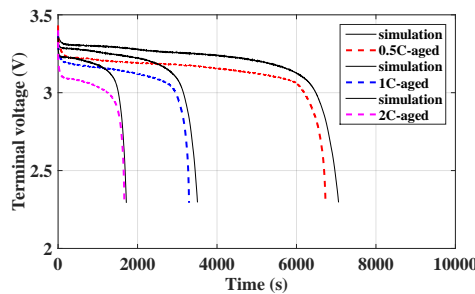


Fig. 13. The results of experiments performed on an aged LiFePO₄ battery.

Remark A-3. Like other optimization methods, EAs also require an objective function, which is often called the fitness function. Even if the closed-form expression of the fitness function is unknown, it can be used to indicate how good a candidate solution is. As shown in the following figure, the error e between model output \hat{U} and reference voltage U^{ref} is considered as the objective function value in our method.

Note that the output of the P2D model can be obtained directly from the model simulation performed in COMSOL. Thus, the accurate mathematical relationship $f(\vec{\theta})$ between candidate parameters and model output is not required. It is the reason that the proposed method can be used without the closed-form expression of the objective function.

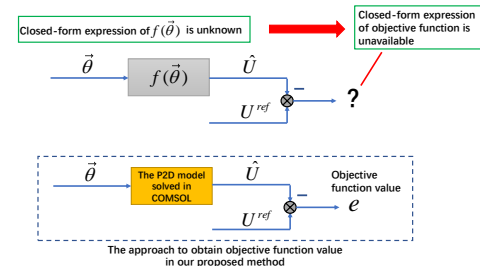


Fig. 14. The approach to obtain objective function value in the proposed method.

REFERENCES

- [1] J. Shen, S. Dusmez, and A. Khaligh, "Optimization of sizing and battery cycle life in battery/ultracapacitor hybrid energy storage systems for electric vehicle applications," *IEEE Transactions on Industrial Informatics*, vol. 10, no. 4, pp. 2112–2121, 2014.
- [2] S. Xie, S. Qi, and K. Lang, "A data-driven power management strategy for plug-in hybrid electric vehicles including optimal battery depth of discharging," *IEEE Transactions on Industrial Informatics*, pp. 1–1, 2019.
- [3] Z. Liu and H. Li, "A spatiotemporal estimation method for temperature distribution in lithium-ion batteries," *IEEE Transactions on Industrial Informatics*, vol. 10, no. 4, pp. 2300–2307, 2014.
- [4] X. Hu, R. Xiong, and B. Egardt, "Model-based dynamic power assessment of lithium-ion batteries considering different operating conditions," *IEEE Transactions on Industrial Informatics*, vol. 10, no. 3, pp. 1948–1959, 2014.
- [5] S. Muhammad, M. U. Rafique, S. Li, Z. Shao, Q. Wang, and N. Guan, "A robust algorithm for state-of-charge estimation with gain optimization," *IEEE Transactions on Industrial Informatics*, vol. 13, no. 6, pp. 2983–2994, 2017.
- [6] G. H. Hui, P. Ji, S. S. Mi, and S. P. Deng, "Electrochemical impedance spectrum frequency optimization of bitter taste cell-based sensors," *Biosensors & Bioelectronics*, vol. 47, no. 18, pp. 164–170, 2013.
- [7] L. Liu, J. Park, X. Lin, A. M. Sastry, and W. Lu, "A thermal-electrochemical model that gives spatial-dependent growth of solid electrolyte interphase in a li-ion battery," *Journal of Power Sources*, vol. 268, no. 4, pp. 482–490, 2014.
- [8] H. Lin, T. Liang, and S. Chen, "Estimation of battery state of health using probabilistic neural network," *IEEE Transactions on Industrial Informatics*, vol. 9, no. 2, pp. 679–685, 2013.
- [9] P. Kemper, S. E. Li, and D. Kum, "Simplification of pseudo two dimensional battery model using dynamic profile of lithium concentration," *Journal of Power Sources*, vol. 286, pp. 510–525, 2015.
- [10] A. Jokar, B. Rajabloo, M. Désilets, and M. Lacroix, "Review of simplified pseudo-two-dimensional models of lithium-ion batteries," *Journal of Power Sources*, vol. 327, pp. 44–55, 2016.
- [11] C. Fleischer, W. Waag, H. M. Heyn, and D. U. Sauer, "On-line adaptive battery impedance parameter and state estimation considering physical principles in reduced order equivalent circuit battery models: Part 2. parameter and state estimation," *Journal of Power Sources*, vol. 262, no. sep.15, pp. 457–482.
- [12] A. Singh, A. Izadian, and S. Anwar, "Model based condition monitoring in lithium-ion batteries," *Journal of Power Sources*, vol. 268, pp. 459–468.
- [13] V. Boovaragavan, S. Harinipriya, and V. R. Subramanian, "Towards real-time (milliseconds) parameter estimation of lithium-ion batteries using reformulated physics-based models," *Journal of Power Sources*, vol. 183, no. 1, pp. 361–365, 2008.
- [14] ———, "Towards real-time (milliseconds) parameter estimation of lithium-ion batteries using reformulated physics-based models," *Journal of Power Sources*, vol. 183, no. 1, pp. p.361–365.

- [15] B. Rajabloo, A. Jokar, M. Désilets, and M. Lacroix, "An inverse method for estimating the electrochemical parameters of lithium-ion batteries," *Journal of the Electrochemical Society*, vol. 164, no. 2, pp. A99–A105, 2017.
- [16] M. Kim, H. Chun, J. Kim, K. Kim, J. Yu, T. Kim, and S. Han, "Data-efficient parameter identification of electrochemical lithium-ion battery model using deep bayesian harmony search," *Applied Energy*, vol. 254, p. 113644, 2019.
- [17] J. Li, L. Zou, F. Tian, X. Dong, Z. Zou, and H. Yang, "Parameter identification of lithium-ion batteries model to predict discharge behaviors using heuristic algorithm," *Journal of the Electrochemical Society*, vol. 163, no. 8, pp. A1646–A1652, 2016.
- [18] Y. Oka and M. Ohno, "Parameter estimation for heat transfer analysis during casting processes based on ensemble kalman filter," *International Journal of Heat and Mass Transfer*, vol. 149, p. 119232, 2020.
- [19] R. H. Reichle, D. McLaughlin, and D. Entekhabi, "Hydrologic data assimilation with the ensemble kalman filter," *Monthly Weather Review*, vol. 130, no. 1, pp. 103–114, 2002.
- [20] H. L. Mitchell, P. L. Houtekamer, and G. Pellerin, "Ensemble size, balance, and model-error representation in an ensemble kalman filter*," *Monthly Weather Review*, vol. 130, no. 11, pp. 2791–2808, 2002.
- [21] I. Z. M. Darus and Tokhi, "Parametric and non-parametric identification of a two dimensional flexible structure," *Journal of Low Frequency Noise Vibration and Active Control*, vol. 25, no. 2, pp. 119–143, 2006.
- [22] M. A. Rahman, S. Anwar, and A. Izadian, "Electrochemical model parameter identification of a lithium-ion battery using particle swarm optimization method," *Journal of Power Sources*, vol. 307, pp. 86–97, 2016.
- [23] P. W. C. Northrop, "Multiscale modeling, reformulation, and efficient simulation of lithium-ion batteries," *Dissertations & Theses - Gradworks*, 2014.
- [24] L. Cai and R. E. White, "Mathematical modeling of a lithium ion battery with thermal effects in comsol inc. multiphysics (mp) software," *Journal of Power Sources*, vol. 196, no. 14, pp. 5985–5989, 2011.
- [25] B.-C. Wang, H.-X. Li, and Y. Feng, "An improved teaching-learning-based optimization for constrained evolutionary optimization," *Information Sciences*, vol. 456, pp. 131–144, 2018.
- [26] N. H. Luong, H. La Poutré, and P. A. Bosman, "Multi-objective gene-pool optimal mixing evolutionary algorithm with the interleaved multi-start scheme," *Swarm and Evolutionary Computation*, vol. 40, pp. 238–254, 2018.
- [27] L. Zhang, L. Wang, G. Hinds, C. Lyu, J. Zheng, and J. Li, "Multi-objective optimization of lithium-ion battery model using genetic algorithm approach," *Journal of Power Sources*, vol. 270, pp. 367–378, 2014.
- [28] T. F. Fuller, M. Doyle, and J. Newman, "Simulation and optimisation of the dual lithium ion insertion cell," *Journal of the Electrochemical Society*, vol. 141, no. 1, pp. 1–10, 1993.
- [29] M. Doyle, J. Newman, A. S. Gozdz, C. N. Schmutz, and J. M. Tarascon, "Comparison of modeling predictions with experimental data from plastic lithium ion cells," *Journal of The Electrochemical Society*, vol. 143, no. 6, pp. 1890–1903, 1996.
- [30] A. Jokar, B. Rajabloo, M. Desilets, and M. Lacroix, "An inverse method for estimating the electrochemical parameters of lithium-ion batteries i. methodology," *Journal of The Electrochemical Society*, vol. 163, no. 14, 2016.
- [31] D. R. Jones, M. Schonlau, and W. J. Welch, "Efficient global optimization of expensive black-box functions," *Journal of Global Optimization*, vol. 13, no. 4, pp. 455–492, 1998.
- [32] B. Liu, H. Yang, and M. J. Lancaster, "Global optimization of microwave filters based on a surrogate model-assisted evolutionary algorithm," *IEEE Transactions on Microwave Theory and Techniques*, pp. 1–10.
- [33] M. T. M. Emmerich, K. C. Giannakoglou, and B. Naujoks, "Single- and multiobjective evolutionary optimization assisted by gaussian random field metamodels," *IEEE Transactions on Evolutionary Computation*, vol. 10, no. 4, pp. 421–439, 2006.
- [34] M. Hamzeh, B. Vahidi, and A. F. Nematollahi, "Optimizing configuration of cyber network considering graph theory structure and teaching-learning-based optimization (gt-lbo)," *IEEE Transactions on Industrial Informatics*, vol. 15, no. 4, pp. 2083–2090, 2019.
- [35] M. D. McKay, R. J. Beckman, and W. J. Conover, "A comparison of three methods for selecting values of input variables in the analysis of output from a computer code," *Technometrics*, vol. 42, no. 1, pp. 55–61, 2000.
- [36] A. O. S. Dahlblom, "On latin hypercube sampling for structural reliability analysis," *Structural Safety*, 2003.
- [37] A. I. J. Forrester and A. J. Keane, "Recent advances in surrogate-based optimization," *Progress in Aerospace Sciences*, vol. 45, no. 1, pp. 50–79, 2009.
- [38] D. R. Jones, "A taxonomy of global optimization methods based on response surfaces," *Journal of Global Optimization*, vol. 21, no. 4, pp. 345–383, 2001.
- [39] D. D. Cox and S. John, "A statistical method for global optimization," in *IEEE International Conference on Systems*, 1992.
- [40] J. Schoukens, Y. Rolain, and R. Pintelon, "On the use of parametric and non-parametric noise-models in time- and frequency domain system identification," in *Decision and Control (CDC), 2010 49th IEEE Conference on*, 2011.
- [41] L. Ljung, "Convergence analysis of parametric identification methods," *IEEE Transactions on Automatic Control*, vol. 23, no. 5, pp. 770–783, 1978.
- [42] B. Balagopal and M. Y. Chow, "Effect of anode conductivity degradation on the thevenin circuit model of lithium ion batteries," in *Conference of the IEEE Industrial Electronics Society*, 2016.
- [43] J. Li, Y. Cheng, L. Ai, M. Jia, S. Du, B. Yin, S. Woo, and H. Zhang, "3d simulation on the internal distributed properties of lithium-ion battery with planar tabbed configuration," *Journal of Power Sources*, vol. 293, no. 293, pp. 993–1005, 2015.
- [44] T. M. Bandhauer, S. Garimella, and T. F. Fuller, "A critical review of thermal issues in lithium-ion batteries," *Journal of The Electrochemical Society*, vol. 158, no. 3, 2011.
- [45] A. Gupta, Y. Ong, and L. Feng, "Insights on transfer optimization: Because experience is the best teacher," *IEEE Transactions on Emerging Topics in Computational Intelligence*, vol. 2, no. 1, pp. 51–64, 2018.



Yu Zhou received the B.E. degree in mechanical engineering from Hunan Normal University, Changsha, China, in 2017. He is currently working on his joint Ph.D. degree in Central South University and City University of Hong Kong. His current research interests include lithium-ion battery modeling, optimization, and estimation.



Bing-Chuan Wang received the B.E. degree in automation and the M.S. degree in control science and engineering both from Central South University, Changsha, China, in 2013 and 2016, respectively. He received the Ph.D. degree from the City University of Hong Kong, Hong Kong. From 2020, Dr. Wang is with the School of Automation, Central South University. His current research interests include intelligent modeling and evolutionary computation.



Han-Xiong Li (S'94-M'97-SM'00-F'11) received his B.E. degree in aerospace engineering from the National University of Defense Technology, China in 1982, M.E. degree in electrical engineering from Delft University of Technology, The Netherlands in 1991, and Ph.D. degree in electrical engineering from the University of Auckland, New Zealand in 1997. He is a professor in the Department of SEEM, City University of Hong Kong. He has a broad experience in both academia and industry. He has authored 2 books and about 20 patents, and published more than 200 SCI journal papers with h-index 48 (web of science). His current research interests include process modeling and control, distributed parameter systems, and system intelligence.

Dr. Li serves as Associate Editor for IEEE Transactions on SMC: System, and was associate editor for IEEE Transactions on Cybernetics (2002–2016) and IEEE Transactions on Industrial Electronics (2009–2015). He was awarded the Distinguished Young Scholar (overseas) by the China National Science Foundation in 2004, a Chang Jiang professorship by the Ministry of Education, China in 2006, and a national professorship in China Thousand Talents Program in 2010. He serves as a distinguished expert for Hunan Government and China Federation of Returned Overseas Chinese. He is a Fellow of the IEEE.